Quantifying hydrogen peroxide in iron-containing solutions using leuco crystal violet

Corey A. Cohn[a)]
Department of Geosciences and Center for Environmental Molecular Science, Stony Brook University, Stony Brook, New York 11794-2100

Aimee Pak
Department of Chemistry and Center for Environmental Molecular Science, Stony Brook University, Stony Brook, New York 11794-2100

Daniel Strongin
Department of Chemistry, Beury Hall 201, 1901 North 13th Street, Temple University, Philadelphia, Pennsylvania 19122 and Center for Environmental Molecular Science, Stony Brook University, Stony Brook, New York 11794-2100

Martin A. Schoonen
Department of Geosciences and Center for Environmental Molecular Science, Stony Brook University, Stony Brook, New York 11794-2100

(Received 24 February 2005; accepted 26 April 2005; published 14 June 2005)

Hydrogen peroxide is present in many natural waters and wastewaters. In the presence of Fe(II), this species decomposes to form hydroxyl radicals, that are extremely reactive. Hence, in the presence of Fe(II), hydrogen peroxide is difficult to detect because of its short lifetime. Here, we show an expanded use of a hydrogen peroxide quantification technique using leuco crystal violet (LCV) for solutions of varying *p*H and iron concentration. In the presence of the biocatalyst peroxidase, LCV is oxidized by hydrogen peroxide, forming a colored crystal violet ion (CV^+), which is stable for days. The LCV method uses standard equipment and allows for detection at the low microM concentration level. Results show strong *p*H dependence with maximum LCV oxidation at *p*H 4.23. By chelating dissolved Fe(II) with EDTA, hydrogen peroxide can be stabilized for analysis. Results are presented for hydrogen peroxide quantification in pyrite–water slurries. Pyrite–water slurries show surface area dependent generation of hydrogen peroxide only in the presence of EDTA, which chelates dissolved Fe(II). Given the stability of CV^+, this method is particularly useful for field work that involves the detection of hydrogen peroxide. © *2005 American Institute of Physics*. [DOI: 10.1063/1.1935449]

INTRODUCTION

Hydrogen peroxide is an important reactant in natural aquatic systems, environmental remediation technologies, and in biological systems. Reactive oxygen species (ROS), which include hydrogen peroxide (H_2O_2) and hydroxyl radicals ($^{\cdot}OH$) occur in rain[1,2] and surface waters.[3,4] ROS play an important role in natural processes in aquatic systems, including, radiolysis,[5,6] pyrite oxidation,[7–9] and photochemical oxidation.[10,11] Hydrogen peroxide also is intentionally added to wastewaters to promote *in situ* oxidation processes[12,13] by leveraging the extreme reactivity of radicals toward organic pollutants. The generation of $^{\cdot}OH$, via the decomposition of H_2O_2, degrades contaminants when methods involving microbiological degradation are ineffective. In organisms, including humans, ROS are produced during metabolic and immune system function.[14] When ROS concentrations are above normal for prolonged periods of time, however, their presence can lead to oxidative stress.[15] Oxidative stress is now recognized to be an important factor in the development or enhancement of many diseases.[16]

Among ROS, H_2O_2 is relatively stable,[17] in the presence of ferrous iron, H_2O_2 forms $^{\cdot}OH$ via the Fenton reaction

$$\mathrm{Fe(II)} + \mathrm{H_2O_2} \rightarrow {}^{\cdot}\mathrm{OH} + \mathrm{OH^-} + \mathrm{Fe(III)}. \quad (1)$$

$^{\cdot}OH$ is far more reactive than H_2O_2 and its reaction with aqueous species is diffusion limited.[17] Therefore, H_2O_2, in the presence of Fe(II), represents great potential for reactivity.

In natural systems, $^{\cdot}OH$ is a transient species and its steady-state concentration may only be in the nM range. The inherent reactivity of $^{\cdot}OH$ precludes its detection via a direct measurement, and hence, methods generally rely on the detection of a stable reaction product resulting from the reaction of $^{\cdot}OH$ and a target molecule. One strategy is to add a reactant as a target species that will oxidize in the presence of $^{\cdot}OH$ and form a product that can be analyzed by UV–Vis spectroscopy[2] or fluorescence.[18] Verifying $^{\cdot}OH$ involvement in oxidation of the target species is difficult. Addition of competing scavengers that react with $^{\cdot}OH$ may inhibit oxidation of the target molecule; however, there is little conformity when using different scavengers and target molecules.[19] Another strategy that is often employed is to "trap" the unpaired electron of the radical into a compound that is less

a)Author to whom correspondence should be addressed; electronic mail: ccohn@fulbrightweb.org

reactive. By using electron paramagnetic resonance (EPR), the EPR intensity of the spin-trapped molecule can be directly related to the concentration of $^{\cdot}OH$ in the solution. EPR spin-trapping is a very sensitive technique and has been widely used in chemistry, environmental sciences, and bio-(medical) sciences; however, it does require a significant capital investment and spin-trapping cannot be conducted in the field. The spin-trapping technique has also been used for $^{\cdot}OH$ detection from aqueous mineral slurries, however reaction between Fe(III) and the spin-trap complicates interpretation of the data.[20]

Where detection of $^{\cdot}OH$ is impracticable, identifying H_2O_2 may elucidate a reaction mechanism involving $^{\cdot}OH$ formation. In iron-containing systems, both H_2O_2 and $^{\cdot}OH$ are short-lived. However, chelation of iron [i.e., Fe(II)] avoids its interaction and decomposition of H_2O_2. Hence, we argue that hydrogen peroxide detected in iron-containing systems with an iron-chelator added is a proxy for the capacity of the system to generate $^{\cdot}OH$ in the absence of an iron chelator. This strategy may prove useful as an alternative method for radical detection in natural systems.

Several methods are available for quantifying H_2O_2. UV–Vis absorbance (240 nm, ϵ=43.6 M^{-1} cm^{-1})[21] is convenient for H_2O_2 solutions containing no other UV absorbing chromophores. Another spectrophotometric method uses copper(II) and 2,9-dimethyl-1,10-phenanthroline (DMP) for μM H_2O_2 detection in wastewater.[22] The colored complex does not change in the presence of humic acid; however, metal chelators affect the copper reactivity, complicating its use when iron chelation is necessary. For higher sensitivity detection, fluorometric techniques are available. The scopoletin/horseradish peroxidase method[23] allows for detection of low nM concentrations, but the need for standard additions and quantification via a decrease in fluorescence prove to be time consuming. Another fluorometric technique involves the oxidation of non-fluorescent 2′,7′-dichlorofluorescin (DCFH) to fluorescent 2′,7′-dichlorofluorescein (DCF) in the presence of H_2O_2 and peroxidase.[18] This technique is often used to detect the formation of H_2O_2 in cells. The technique makes use of the non-fluorescent (DCFH-diacetate) crossing of cell membranes, which is enzymatically deacetylated to non-fluorescent DCFH. Cellular production of H_2O_2 produces the fluorescent DCF. The deacetylation process can be achieved chemically, but H_2O_2 may be produced in the process,[24] resulting in background levels of H_2O_2. Another disadvantage for using the DCFH technique is the necessity for daily preparation of the DCFH reagent.

Here, we present results on an improved method for H_2O_2 detection in the μM to several hundred nM range, which has several advantages over preexisting methods. The leuco crystal violet (LCV) method[25] involves oxidation of 4,4′4″-methylidynetris (*N*,*N*-dimethylaniline) ($C_{25}H_{31}N_3$) (LCV) in the presence of H_2O_2 and horseradish peroxidase (HRP) to form the crystal violet ion, CV^+, which absorbs at 590 nm. CV^+ remains stable for several days, which makes it possible to treat samples upon collection and perform the analysis at a later time. This is of value in field studies or shipboard analysis.[26] Daily preparation of new reagents is not required and iron chelators do not affect the analysis.

In this report, the LCV method was employed for analysis of H_2O_2 in pyrite/aqueous slurries. Recently,[9] pyrite (FeS_2), the most abundant metal sulfide mineral on Earth, has been shown to produce H_2O_2 in aqueous solutions. Several adjustments were made to the original LCV method so that it is now possible to determine H_2O_2 concentration in aqueous systems that contain iron-bearing minerals. Here, we determined effects of iron, *p*H, and addition of EDTA. To verify that our technique was specific to the presence of H_2O_2, and that other species were not responsible for the oxidation of LCV in the presence of HRP, we carried out experiments in the presence of catalase. This enzyme selectively decomposes H_2O_2, and its addition to the solution prior to the addition of LCV and HRP eliminates the production of the CV^+ species.

EXPERIMENT

Leuco crystal violet (Spectrum) in the presence of the enzyme horseradish peroxidase (HRP) type II (Aldrich) forms a crystal violet cation, which has an absorbance maximum at 590 nm. The absorbance of CV^+ was measured with a Hach DR4000 spectrometer interfaced with a laptop for data storage. Calibration curves were used to quantify the effects of *p*H, iron (Fisher brand ferrous ammonium sulfate), and EDTA (Sigma) on the absorbance of CV^+. Catalase (Sigma 40 000 to 60 000 units/mg bovine liver) was used at a concentration around 100 000 units per sample vial to verify the presence of H_2O_2. Pyrite (Wards brand from Huanzala, Peru) was crushed and sieved under an ambient atmosphere, acid washed (0.1 M HCl), and then thoroughly rinsed with N_2-purged water (Easy Pure 18.3 MΩ cm, UV-irradiated, and ultrafiltered) under N_2 atmosphere to remove surface oxides. The acid-washed and cleaned pyrite was subsequently dried in a vacuum desiccator and stored under vacuum. The size fraction used in these experiments was between 10 and 90 μm with a five point N_2 adsorption BET surface area of roughly 1.25 m^2/g. This BET surface area is an approximation due to the inherent variations for low surface area measurements.[27] Varying amounts of the pyrite were mixed with water in the absence or presence of 1–10 mM EDTA, then immediately filtered (Millipore 0.45 μm). Reagents [all stored at 4 °C and brought up to room temperature (22±1 °C) before analyses] were added to the aqueous filtrate in the following order for a total volume of 2 ml (also shown in Table I): 100 mM KH_2PO_4 (Aldrich) *p*H 4 buffer, 41 μM leuco crystal violet (dissolved with HCl), and 4 mg/50 ml HRP [containing 1.5 mM azide (Sigma) to prevent bacterial growth]. Samples were kept in the dark at room temperature (22±1 °C) for 30 min, upon which absorbance stabilized. Absorbance measurements were taken in 1 cm path-length cuvettes.

RESULTS AND DISCUSSION

The reagent preparations and volumes used are shown in Table I. It is useful to present our conditions in the context of prior LCV studies that were carried out by Zhang *et al.*[26]

TABLE I. LCV method details.[a]

Reagent	Reagent preparation	Stock concentration	Volume added (μl)	Final concentration
Sample[b]	⋯	⋯	1700	⋯
KH_2PO_4 *p*H buffer	136.07 g+0.5 L H_2O, *p*H adjusted to 4.2 with H_3PO_4	1 M	200	100 mM
LCV	31 mg LCV+30 ml H_2O+19.2 ml of 0.25 N HCl	1.65 mM	50	41 μM
HRP	4.0 mg HRP+50 ml H_2O+92 μl of 1 M sodium azide	0.08 mg/ml (14.4 units/ml)	50	1 μg (0.18 units)

[a]Reagent preparations, concentrations, volume added, and final concentrations of the solutions added to a 4 ml cuvette and kept in the dark before analysis. Reagents listed in order of addition. H_2O_2 calibration solutions were prepared by dilutions of a stock.
[b]Samples containing pyrite were filtered.

Compared to the concentrations used by Zhang *et al.* for *p*H buffer, LCV, and HRP, we used 1.25, 4, and 10 times those previously used, respectively, to increase (1) the buffer concentration, (2) the higher range of detection (more LCV), and (3) the reaction rate (more HRP). By increasing the concentration of our reagents, we were able to limit the volume of reagent addition so that a maximum volume would be available for the sample.

Figure 1 shows color development over time after the last reagent, HRP, is added to hydrogen peroxide and LCV. Absorbance levels plateau in 5–10 min and remain stable for several days. Zhang *et al.*[26] waited 5 min before taking absorbance measurements; we waited 30 min just as a cautionary measure to ensure stability of the absorbance. The inset is a plot of wavelength scans showing maximum absorbance at 590 nm and an overlapping of scans after 2 min. Absorbance measurements at 590 nm (A_{590}) were taken at 30 min for all other samples.

Addition of catalase is important for verifying the presence of H_2O_2, since other ROS or other reactions may also oxidize LCV. When catalase is added, no H_2O_2 is detected, which limits the possibility of false positives.

The LCV method is strongly affected by *p*H, and Fig. 2 shows A_{590} as a function of *p*H. The optimal *p*H range is 3.6–4.2, where the peak intensity is the highest, but the intensity decreases by half as the *p*H increases to 4.37 (Fig. 2). Zhang *et al.*[26] have shown a similar increase in absorbance up to around *p*H 4.5. They report CV^+ precipitation at higher *p*H, and here, the effect at *p*H greater than 4.5 is shown. Although A_{590} is significantly reduced and the solutions are slightly turbid, calibration curves can still be produced and H_2O_2 quantified.

Figure 3 shows calibration curves made between *p*H 2.99 and 3.75 with 0–24 μM H_2O_2. At *p*H values of 3.20 and less, the method is not valid. In the *p*H range of 3.38–3.55, the calibration curves are only useful at low H_2O_2 concentrations. At *p*H 3.64 and 3.75, the curves are nearly linear. These results are consistent with those presented in Fig. 1, which showed the optimal *p*H range of around 3.6–4.2; here, the calibration curves are nearly linear at *p*H 3.64 and 3.75. Above *p*H 3.75, the slopes are expected to be linear (results from higher-*p*H experiments are presented in the following). In separate experiments, which are not shown, calibration curves were extended into the nM region indicating a lower limit around 0.5 μM.

In the presence of Fe(II), EDTA is necessary for stabilizing H_2O_2. As solution *p*H is increased, EDTA is deprotonated, therefore having a higher capacity for chelation (the EDTA stock solution is *p*H 8). In our experiments, 1 mM EDTA with LCV reagents resulted in a *p*H around 3.67. At this *p*H, calibration curves with EDTA are equivalent to those without EDTA. Figure 4 shows the effect of iron on A_{590} at several H_2O_2 concentrations in the presence of 1 mM EDTA. Even without H_2O_2, EDTA and iron oxidize LCV in the presence of HRP. This may be due to reaction of

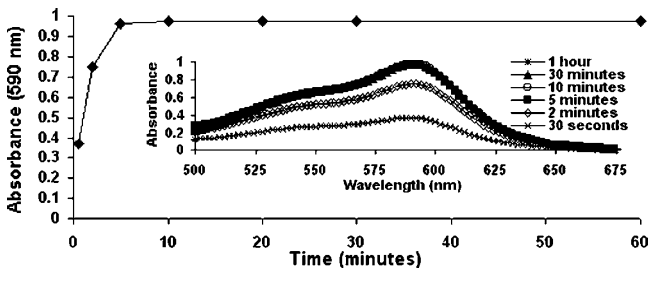

FIG. 1. Oxidation of LCV in the presence of 20 μM H_2O_2 and HRP as a function of time after addition of all reagents. Insert shows wavelength scans of the solutions showing maximum absorbance at 590 nm.

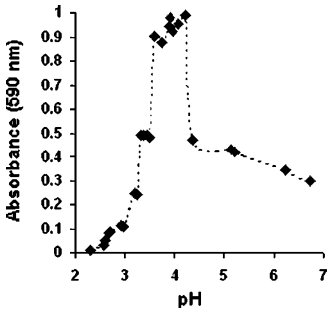

FIG. 2. Absorbance of the buffered LCV and HRP solution as a function of *p*H in the presence of 20 μM H_2O_2.

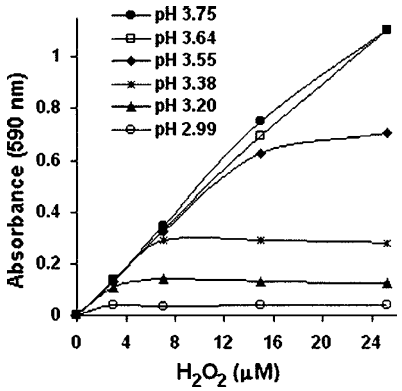

FIG. 3. Calibration curves as a function of *p*H. H_2O_2 quantification using Beer's law is only applicable at $H_2O_2 \lesssim 12$ μM for *p*H=3.55 and $\lesssim 6$ μM for *p*H=3.38.

LCV with either the electron-deficient chelated iron or iron-EDTA complex. When ferrous iron is added at low concentrations (0–15 μM) there is an increase in absorbance but the A_{590} is not affected as the iron concentration is increased above 15 μM iron. At low iron concentrations (0–15 μM), the slopes of the calibration curves are nearly identical to those calculated from experiments without EDTA and iron. As iron is increased, H_2O_2 decreases. This experimental observation is due to a higher proportion of nonchelated iron, which reacts with H_2O_2. Although some of the H_2O_2 was decomposed in the presence of iron, linear calibration curves can still be generated. In these experiments, the concentration of EDTA is much greater than that for iron. EDTA chelation capacity decreases with decreasing *p*H. The optimal *p*H for the LCV technique is around 4, which necessitates the addition of high concentrations of EDTA.

Figure 5 shows calibration curves with 10 mM EDTA solutions at varying ferrous iron concentrations. The *p*H of these solutions is between 5.9 and 5.6. The A_{590} does not vary by much as a function of *p*H in this region. Therefore, differences in the curves are due to iron. Compared to the high EDTA concentration, relatively low iron concentrations decompose H_2O_2. This is probably due to the low *p*H where EDTA has a lower chelation capacity. At higher iron concentrations, around 150–200 μM, only the higher H_2O_2 concentrations are detected. The *p*H for EDTA-containing solutions was buffered but the *p*H was not forced to the optimal *p*H of 4.23 because addition of highly acidic buffers alter EDTA chelation capacity and, in the field, it is easier to quantify H_2O_2 by using a *p*H-specific calibration curve than trying to force the *p*H to 4.23.

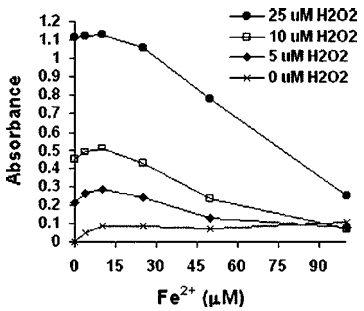

FIG. 4. Effect of dissolved ferrous iron on A_{590} at several H_2O_2 concentrations (given in μm) in the presence of 1 mM EDTA at *p*H=3.67.

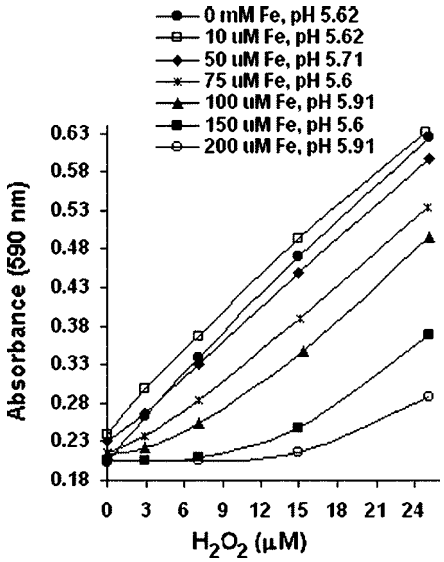

FIG. 5. Calibration curves as a function of ferrous iron (added as ferrous ammonium sulfate, given in μm) in 10 mM EDTA.

Using the DMP method[28] and an ultrahigh vacuum mass spectroscopy technique,[9] pyrite has recently been shown to produce H_2O_2. Here, we used the LCV method and employed EDTA to verify H_2O_2 at several particle loadings (Fig. 6). These results show a surface area dependence on H_2O_2 generation. The H_2O_2 concentrations reported here are about 200 times lower than those obtained previously (34 μM at a 4 g/L loading).[28] The higher readings in the prior study may have been due to the presence of dissolved Fe(II), which enhances H_2O_2 readings with the DMP method. The DMP method uses Cu, so EDTA would interfere with the analysis. Hence the values reported in our earlier work based on the DMP method are overestimated.

Addition of catalase to the solution prior to the addition of LCV results in a colorless solution, suggesting that hydrogen peroxide was not present upon addition of LCV and HRP (Fig. 7). Catalase specifically reacts with H_2O_2, so that it will remove any H_2O_2 from the EDTA-treated solution. By performing two measurements, one with EDTA and one with EDTA plus catalase, we rule out false positives due to other reactions that could conceivably lead to the formation of CV^+. Without EDTA, there is no LCV oxidation, since in this case ferrous iron, either on the pyrite surface or in solution, is not chelated and it can react with hydrogen peroxide to form $^{\cdot}OH$. In a separate study,[29] we have shown that without

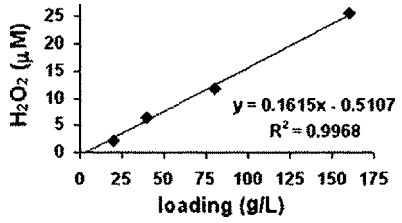

FIG. 6. Pyrite-generated H_2O_2 as a function of particle loadings. 1 mM EDTA was used for the 20 and 40 g/L loadings and 10 mM EDTA was used for the 80 and 160 g/L loadings. The EDTA solutions were quickly mixed with pyrite particles for about 3 s and filtered. LCV and HRP were then added to the filtrate. When catalase is added prior to LCV, H_2O_2 is not detected.

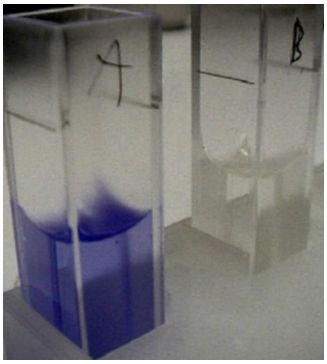

FIG. 7. (Color) Photograph of the cuvettes containing pyrite slurry filtrate and LCV reagents. Both contain 1 mM EDTA. The left cuvette is purple due to CV^+. On the right, catalase was added before addition of LCV. Catalase reacts rapidly with H_2O_2, preventing LCV oxidation and resulting in a colorless solution.

EDTA, pyrite readily degrades biomolecules including RNA, presumably due to hydroxyl radical generation from the reaction of ferrous iron with hydrogen peroxide. This study also showed that addition of EDTA protects the biomolecules, which are only degraded if $^{\cdot}OH$ is formed.

For H_2O_2 detection in natural waters, the LCV technique may be one of the more suitable methods. It has already been shown that the method can be used for seawater analyses[26] and here we show that it can be used for a *p*H range of around 3.5–6.0 and in the presence of EDTA. Compared to techniques involving fluorescence, where reagents are prepared on the day of analyses, our solutions of LCV and HRP remained stable for months at 4 °C in opaque centrifuge vials. The stability of CV^+ upon reaction of H_2O_2 and the LCV reagents makes it possible to quantify H_2O_2 several days after sampling. This can be exploited in field studies. For example, the LCV technique could be used to study the spatial and temporal distribution of H_2O_2 in hot spring waters in Yellowstone National Park. It has been shown that steady-state levels of photochemically produced H_2O_2 in the surface geothermal waters at Yellowstone National Park reach 200–600 nM by late afternoon and decrease to less than 50 nM during the night.[30] With the LCV technique a large number of water samples can be collected and prepared for later analysis. Temperature is expected to affect the rate of the HRP-mediated reaction and it could possibly also affect the stability of the LCV or CV^+. Probably the best strategy working with hydrothermal waters is to rapidly cool the sample down to a temperature between 20 and 30 °C before adding the reagents. Cooling the samples to much lower temperature may impede the enzyme reaction. Further experimental work would be needed to resolve this temperature dependence. The LCV technique may also prove to be useful to evaluate the performance of environmental remediation projects involving the injection of H_2O_2 into contaminated waters. Many groundwaters contain dissolved iron, which could make it difficult to determine the residual H_2O_2 concentration. With the LCV techniques samples can be treated with ETDA and preserved for latter analysis.

CONCLUSION

This study demonstrates a reliable and efficient method for quantifying H_2O_2 from iron-containing mineral slurries and waste by use of separate calibration curves to account for *p*H and iron concentrations. The stability of the colored CV^+ makes this method suitable for the field or when immediate access to a spectrophotometer is not possible. Relative to the concentration of H_2O_2 consumed, the reported[25] high molar absorptivity of 75 000 M^{-1} cm^{-1} for CV^+ makes it possible to determine H_2O_2 at sub-μM concentration levels. In iron-containing systems at low *p*H, hydrogen peroxide reacts to form $^{\cdot}OH$. Under those conditions, the presence of H_2O_2 as an intermediate to $^{\cdot}OH$ formation would be extremely difficult to detect. The LCV technique as outlined provides a relatively simple method to demonstrate the involvement of H_2O_2 under those conditions.

ACKNOWLEDGMENTS

This work was funded by the Department of Energy through grants to D.R.S. and M.A.S., Basic Energy Sciences Grant Nos. DEFG029ER14644 and DEFG0296ER14633, respectively. The Center for Environmental Molecular Science (NSF CHE 0221934) facilitated the contribution of A.P. to this project. C.C. would like to acknowledge support from a National Defence Science and Engineering Fellowship.

[1] J. D. Willey, R. J. Kieber, and R. D. Lancaster, J. Atmos. Chem. **25**, 149 (1996).
[2] B. C. Faust and J. M. Allen, Environ. Sci. Technol. **27**, 1221 (1993).
[3] P. J. Hakkinen, A. M. Anesio, and W. Graneli, Can. J. Fish. Aquat. Sci. **61**, 1520 (2004).
[4] L. J. A. Gerringa, M. J. A. Rijkenberg, K. R. Timmermans, and A. G. J. Buma, Netherlands J. Sea Res. **51**, 3 (2004).
[5] M. Amme *et al.*, Environ. Sci. Technol. **39**, 221 (2005).
[6] F. Clarens *et al.*, Environ. Sci. Technol. **38**, 6656 (2004).
[7] E. Ahlberg and A. E. Broo, Int. J. Min. Process. **47**, 49 (1996).
[8] J. M. Allen, S. Lucas, and S. K. Allen, Envir. Toxicol. Chem. **15**, 107 (1996).
[9] M. J. Borda, A. R. Elsetinow, D. R. Strongin, and M. A. Schoonen, Croat. Chem. Acta **67**, 935 (2003).
[10] W. Stumm and J. J. Morgan, *Aquatic Chemistry: Chemical Equilibria and Rates in Natural Waters*, 3rd ed. (Wiley-Interscience, New York, 1995), p. 1022.
[11] P. Vaughan and N. Blough, Environ. Sci. Technol. **32**, 2947 (1998).
[12] P. R. Gogate and A. B. Pandit, Adv. Environ. Res. **8**, 501 (2004).
[13] M. Arienzo, Chemosphere **39**, 1629 (1999).
[14] W. Dröge, Physiol. Rev. **82**, 47 (2002).
[15] J. Nordberg and E. S. J. Arnér, Free Radic Biol. Med. **31**, 1287 (2001).
[16] T. Finkel and N. J. Holbrook, Nature (London) **408**, 239 (2000).
[17] W. A. Pryor, Annu. Rev. Physiol. **48**, 657 (1986).
[18] C. P. Lebel, H. Ischiropoulos, and S. C. Bondy, Chem. Res. Toxicol. **5**, 227 (1992).
[19] C. C. Winterbourn, Free Radic Biol. Med. **3**, 33 (1987).
[20] K. Makino, T. Hagiwara, A. Hagi, M. Nishi, and A. Murakami, Biochem. Biophys. Res. Commun. **172**, 1073 (1990).
[21] A. G. Hildebrandt and I. Roots, Arch. Biochem. Biophys. **171**, 385 (1975).
[22] K. Kosaka, H. Yamada, S. Matsui, S. Echigo, and K. Shishida, Environ. Sci. Technol. **32**, 3821 (1998).
[23] T. Holm, G. George, and M. Barcelona, Anal. Chem. **59**, 582 (1987).
[24] C. Rota, C. F. Chignell, and R. P. Mason, Free Radic Biol. Med. **27**, 873 (1999).
[25] H. A. Mottola, B. E. Simpson, and G. Gorin, Anal. Chem. **42**, 410 (1970).
[26] L. S. Zhang and G. T. F. Wong, Talanta **41**, 2137 (1994).
[27] S. J. Gregg and K. S. W. Sing, *Adsorption, Surface Area and Porosity* (Academic, London, 1982).
[28] M. Borda, A. Elsetinow, M. Schoonen, and D. Strongin, Astrobiology **1**, 283 (2001).
[29] C. A. Cohn, M. J. Borda, and M. A. Schoonen, Earth Planet. Sci. Lett. **225**, 271 (2004).
[30] C. L. Wilson *et al.*, Environ. Sci. Technol. **34**, 2655 (2000).